Supporting Information

A Redox-Responsive Self-Assembled Nanoprobe for Photoacoustic Inflammation Imaging to Assess Atherosclerotic Plaque Vulnerability

Wen Gao,[†] Xiang Li,[†] Zhenhua Liu,[*,†] Wei Fu,[‡] Yuhui Sun,[†] Wenhua Cao,[†] Lili Tong,[†] and Bo Tang[*,†]

[†]College of Chemistry, Chemical Engineering and Materials Science, Collaborative Innovation Center of Functionalized Probes for Chemical Imaging in Universities of Shandong, Key Laboratory of Molecular and Nano Probes, Ministry of Education, Institute of Biomedical Sciences, Shandong Normal University, Jinan 250014, P. R. China

[‡]Department of Pharmacy, ZiBo Central Hospital, Zibo 255000, P. R. China

Corresponding Author

*E-mail: tangb@sdnu.edu.cn

*E-mail: liuzhenhua@sdnu.edu.cn

Contents:

Part A: Experimental Methods

Materials. All the reagents used were of analytical grade or above. Bovine serum albumin (BSA) was obtained from J&K Chemicals Technology Co. Ltd. Sodium hydroxide (NaOH), Hydrochloric acid (HCl), Ethanol, acetonitrile, dimethylsulfoxide (DMSO), hydrogen peroxide (H_2O_2) were obtained from Sinopharm Chemical Reagent. Co. Ltd. (Shanghai, China). Tris(hydroxymethyl)aminomethane (Tris), Sodium borohydride ($NaBH_4$), Glutathione (GSH) and 3-(4, 5-dimethyl-thiazol-2-yl)-2,5-diphenyltetrazolium bromide (MTT) were purchased from Sigma-Aldrich (St. Louis, MO, USA). Urea was purchased from Macklin (Shanghai, China). Enzyme-Linked Immunosorbent Assays (ELISA) kits were purchased from Elabscience Biotechnology Co. Ltd. Oxidized low density lipoprotein (ox-LDL) was obtained from Guangzhou Yiyuan biotechnology Co. Ltd. Cell culture products, unless mentioned otherwise were purchased from Gibco, Invitrogen. Water was purified with a Sartorius Arium 611 VF system (Sartorius AG, Germany) to a resistivity of 18.2 MΩ·cm.

Characterization. Transmission electron microscopy (TEM) was carried out on a HT7700 electron microscope. Dynamic light scattering measurements were performed on a Malvern Zeta Sizer Nano (Malvern Instruments). Absorption spectra were measured on a U-4100 UV-vis-NIR spectrophotometer (HITACHI, Japan). Loading capacity was measured on a 1200 Infinity II high-performance liquid chromatography. All pH measurements were performed with a pH-3c digital pH-meter (Shanghai LeiCi Device Works, Shanghai, China) with a combined glass calomel electrode. Absorbance in MTT assay and pharmacokinetics study was measured in a microplate reader (RT 6000, Rayto, USA). PA imaging was accomplished using an Endra Nexus 128 (Ann Arbor, Michigan). Imaging flow cytometry analysis was performed using an Image-Stream^X multispectral imaging flow cytometer (Amnis Corporation) with 642 nm excitation. In vivo small animal imaging was performed with Caliper IVIS Lumina III (Caliper Co., USA).

Stability analysis. The BSA-Cy-Mito nanoprobe (0.25 mg/mL) were dissolved into

PBS buffer (pH 7.4), serum (FBS) and cell culture medium (DMEM) and kept for two weeks at 37 ℃. Pictures of different solutions were recorded at day 0 and 14. Changes in size distribution and absorption peak were detected by Malvern Zeta Sizer Nano and UV-vis-NIR spectrophotometer at day 0, 2, 5, 8, 11, and 14.

Cy-3-NO_2 and Mito-NIRHP releasing. To detect the release of Cy-3-NO_2 and Mito-NIRHP from BSA-Cy-Mito, 1 mL of BSA-Cy-Mito (0.25 mg/mL) was packaged in a dialysis bag (MWCO = 10 kDa) and then immersed in 20 mL PBS containing 10% FBS. At different time points (6 h, 12 h, 24 h, 48 h), 0.4 mL of the outside solution was collected and measured by UV-vis-NIR spectrophotometer to determine the concentrations of released Cy-3-NO_2 and Mito-NIRHP.

Cell culture. The murine macrophage RAW 264.7 cells were purchased from the Committee on Type Culture Collection of the Chinese Academy of Sciences. Cells were cultured in DMEM medium with 10% fetal bovine serum and 100 U/mL of 1% antibiotics penicillin/streptomycin and maintained at 37 ℃ in a 5% CO_2/95% air humidified incubator (MCO-15AC, SANYO).

Cytotoxicity assay. RAW 264.7 macrophages were seeded in 96-well plates (10^4 cells/well) and cultured overnight. Then fresh medium containing different concentrations sterilized BSA-Cy-Mito (0, 0.06, 0.125, 0.25, 0.5, 1, 2 mg/mL) was added to each well and incubated for 24 h. Cell viability was evaluated by MTT assay according to the previously reported method.[1-2] Cells incubated with free medium served as a negative control.

Response of BSA-Cy-Mito in ox-LDL-activated macrophages. Intracellular response of BSA-Cy-Mito was further monitored by imaging flow cytometry (IFC). RAW 264.7 macrophages stimulated with ox-LDL (60, 80, 100 μg/mL) were trypsinized and centrifuged (1000*g*) to obtain a pellet of about 10^6 cells in 150 μL PBS. Catalase (100 μM) was used as H_2O_2 inhibitor. Cell images were acquired using ImageStream^X multispectral imaging flow cytometer, collecting 20000 events per sample at 40×

magnifications. A 642 nm wavelength laser was used to excite Mito-NIRHP. The fluorescence images were collected using the 640-745 nm spectral detection channels. Unstained cells were used to compensate fluorescence between channel images on a pixel-by-pixel basis. Cell images were analyzed using IDEAS® image-analysis software (Amnis).

Animals. All animal experiments were carried out according to the guidelines of the Institutional Animal Care and Use Committee (People's Republic of China). ApoE$^{-/-}$ mice (6-8 weeks old, male) were purchased from Changzhou Cavens Laboratory Animal Co. Ltd. (Changzhou, China) and housed under controlled conditions (12/12 h light/dark cycle; humidity 50-60%; 24-25 ℃ room temperature), with free access to water and chow. To induce the development of atherosclerotic lesions, mice were fed with the high fat diet (HFD, 20% fat, 20% sugar, and 1.25% cholesterol) for 16 weeks.

Pharmacokinetics study. Healthy ApoE$^{-/-}$ mice were given an intravenous injection of FITC-labeled BSA-Cy-Mito at 10 mg/kg. At predetermined time intervals, 20 μL of tail vein blood was withdrawn using a tube containing heparin, and the wound was pressed for several seconds to stop the bleeding. Then, fluorescence intensity of FITC-labeled BSA-Cy-Mito in the blood was determined by an RT 6000 microplate reader. The blood circulation half-life ($t_{1/2}$) was calculated from a first order fit of the data.

Plaque-targeting study. Plaque-bearing ApoE$^{-/-}$ mice were randomly divided into four groups (n = 3) and given an intravenous injection of FITC-labeled BSA-Cy-Mito at 10 mg/kg for 1, 2, and 6 h, respectively. Control group of mice was each injected with PBS. The mice were sacrificed at predetermined time after injecting, and biodistribution of BSA-Cy-Mito was monitored by *ex vivo* fluorescence imaging. Aortas and major organs including heart, liver, spleen, lung and kidney were collected and visualized with Caliper IVIS Lumina III as previously reported method.[3-4] The fluorescence signals in each tissue were normalized to the corresponding pre-injection baseline values.

Statistical analysis. Each experiment was performed in triplicate and repeated three

times if not stated otherwise. Data were presented as mean ± SD.

References

(1) Gao, W.; Cao, W.; Sun, Y.; Wei, X.; Xu, K.; Zhang, H.; Tang, B. *Biomaterials* **2015**, *69*, 212-221.

(2) Yuan, Q.; Zhang, Y.; Chen, T.; Lu, D.; Zhao, Z.; Zhang, X.; Li, Z.; Yan, C.; Tan, W. *ACS Nano* **2012**, *6*, 6337-6344.

(3) Gao, W.; Zhao, Y.; Li, X.; Sun, Y.; Cai, M.; Cao, W.; Liu, Z.; Tong, L.; Cui, G.; Tang, B. *Chem. Sci.* **2018**, *9*, 439-445.

(4) Gomes, R. S. N.; Neves, R. P. D.; Cochlin, L.; Lima, A.; Carvalho, R.; Korpisalo, P.; Dragneva, G.; Turunen, M.; Liimatainen, T.; Clarke, K.; Yl ä-Herttuala, S.; Carr, C.; Ferreira, L. *ACS Nano* **2013**, *7*, 3362-3372.

Part B: Supplementary figures

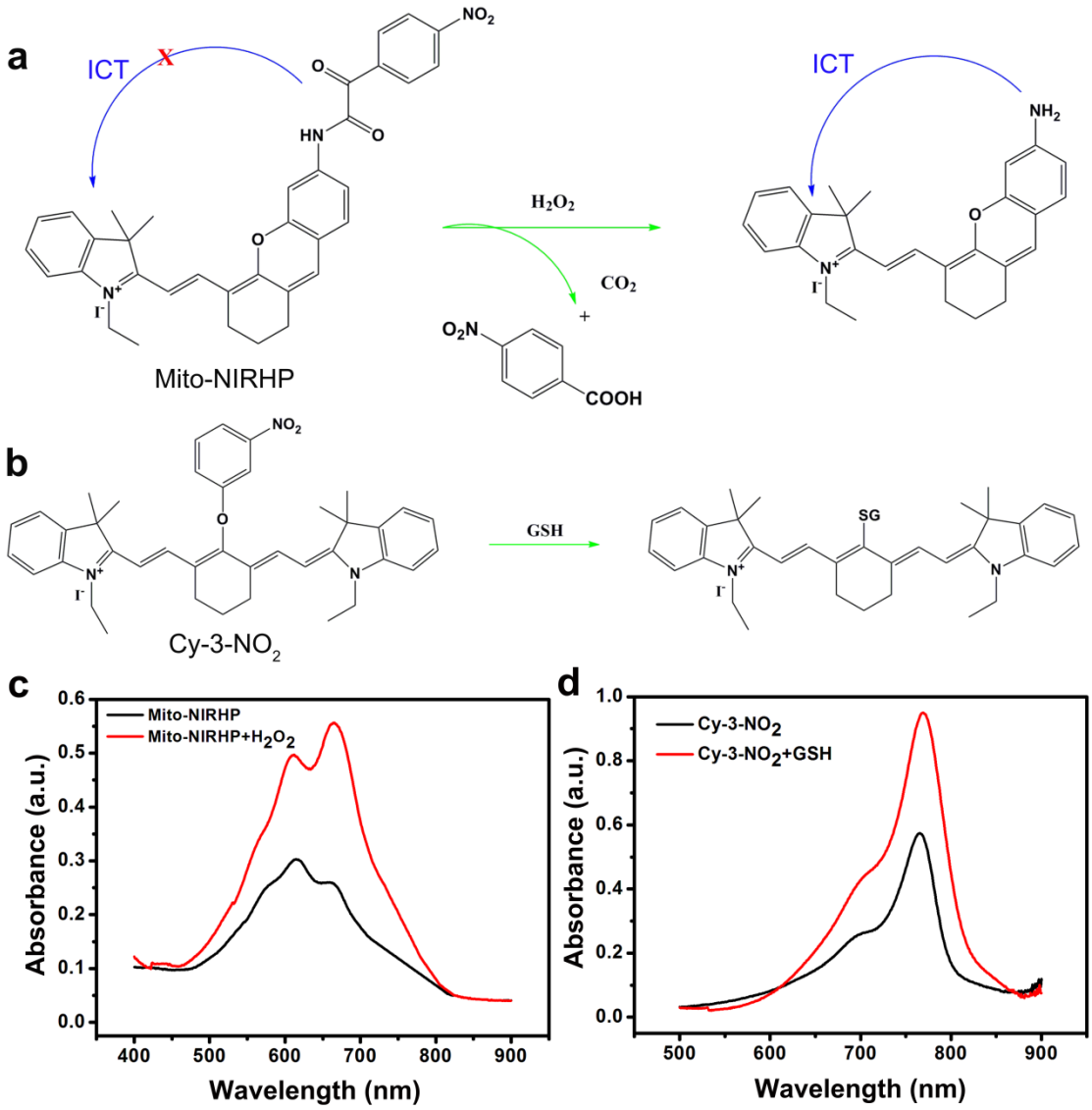

Figure S-1. The proposed reaction mechanism and UV-vis-NIR absorption spectra of (a, c) Mito-NIRHP towards 100 μM of H_2O_2 and (b, d) Cy-3-NO_2 towards 100 μM of GSH.

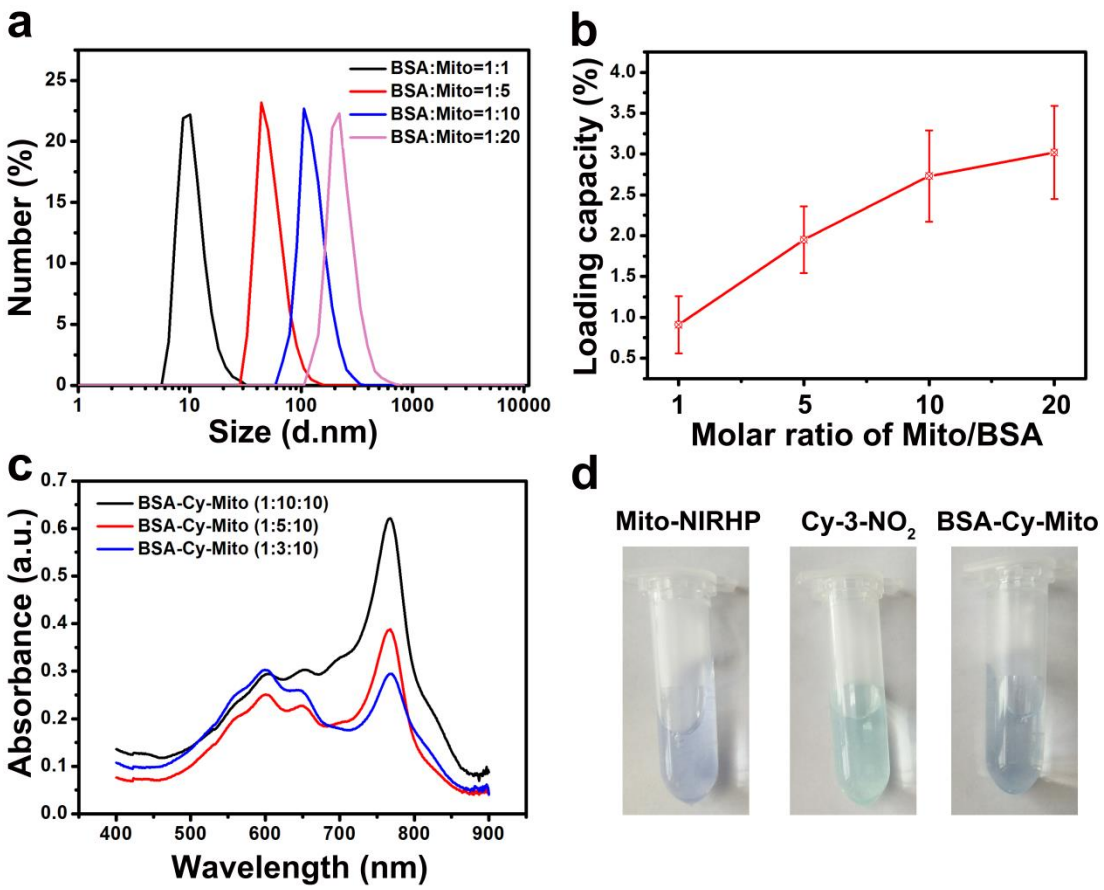

Figure S-2. The optimization of BSA-Cy-Mito nanoprobe. (a) DLS measured diameters of BSA-Mito at different BSA:Mito-NIRHP molar ratios. (b) The loading capacity of Mito-NIRHP obtained at different molar ratios. (c) UV-vis-NIR absorbance spectra of BSA-Cy-Mito prepared at different BSA:Cy-3-NO_2:Mito-NIRHP molar ratios. (d) Photographs of Mito-NIRHP, Cy-3-NO_2, and BSA-Cy-Mito dispersed in PBS (pH 7.4).

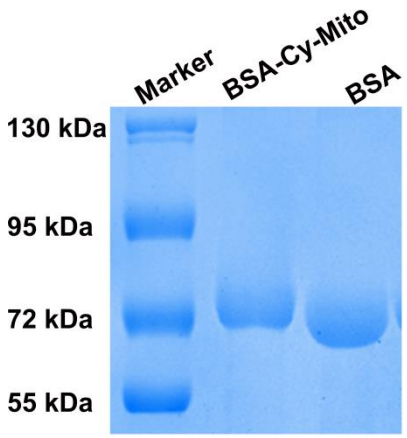

Figure S-3. Gel electrophoresis assay for BSA and BSA-Cy-Mito. BSA (0.25 mg/mL), BSA-Cy-Mito (0.25 mg/mL) were incubated with a loading buffer (5×) at 100 ℃ for 5 min and loaded onto the 8% SDS-PAGE gel.

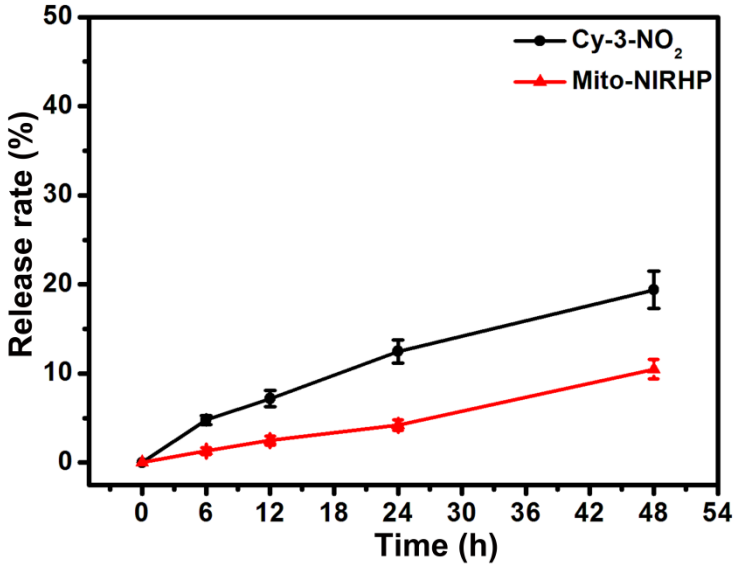

Figure S-4. The time-dependent release profiles of Cy-3-NO_2 and Mito-NIRHP from BSA-Cy-Mito in PBS with 10% FBS.

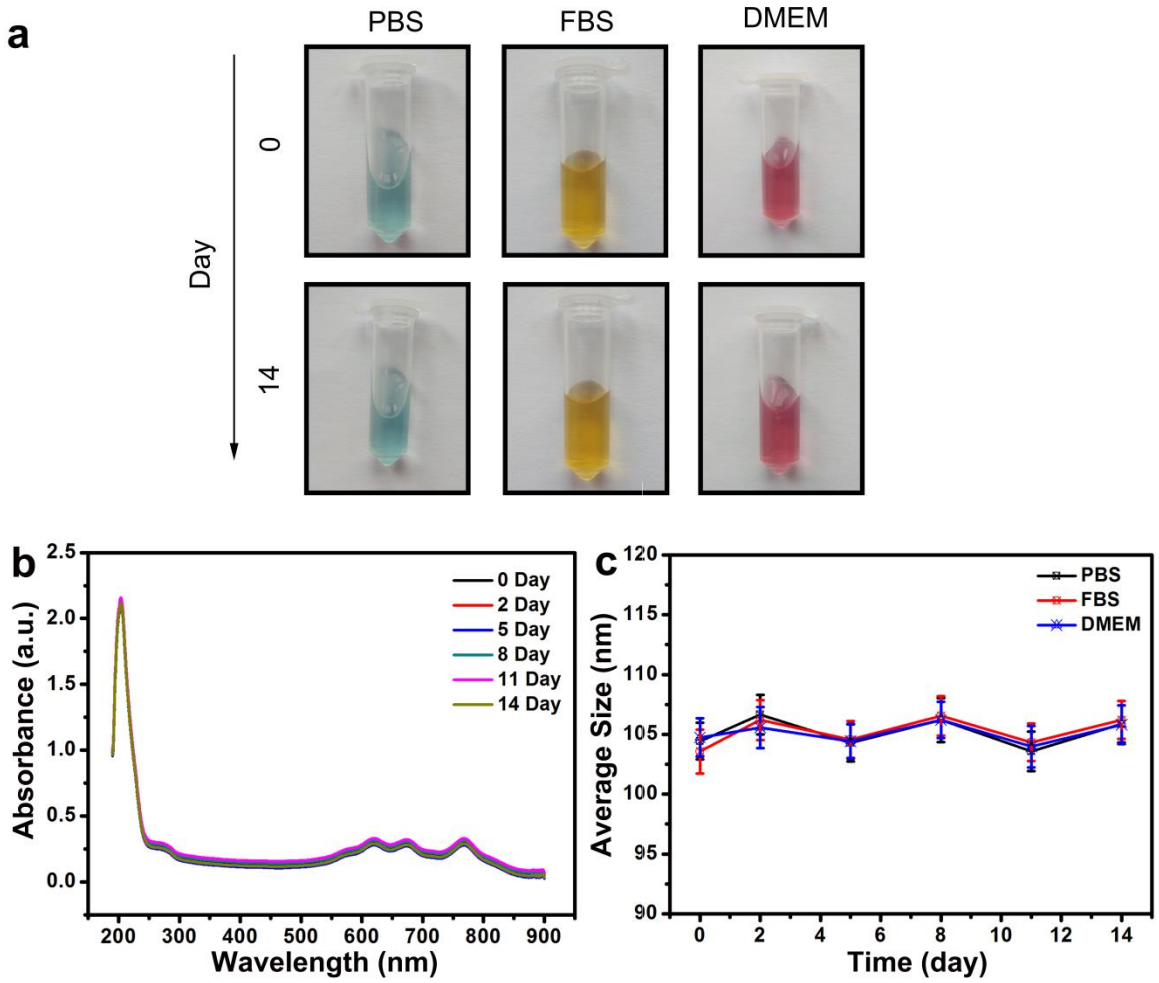

Figure S-5. The stability of BSA-Cy-Mito nanoprobe (a) Photographs of the nanoprobe (0.25 mg/mL) dispersed in PBS, FBS or DMEM for 14 days. (b) UV-vis-NIR absorbance spectra of BSA-Cy-Mito dispersed in PBS for 14 days. (c) DLS data of BSA-Cy-Mito dispersed in PBS, FBS or DMEM for 14 days.

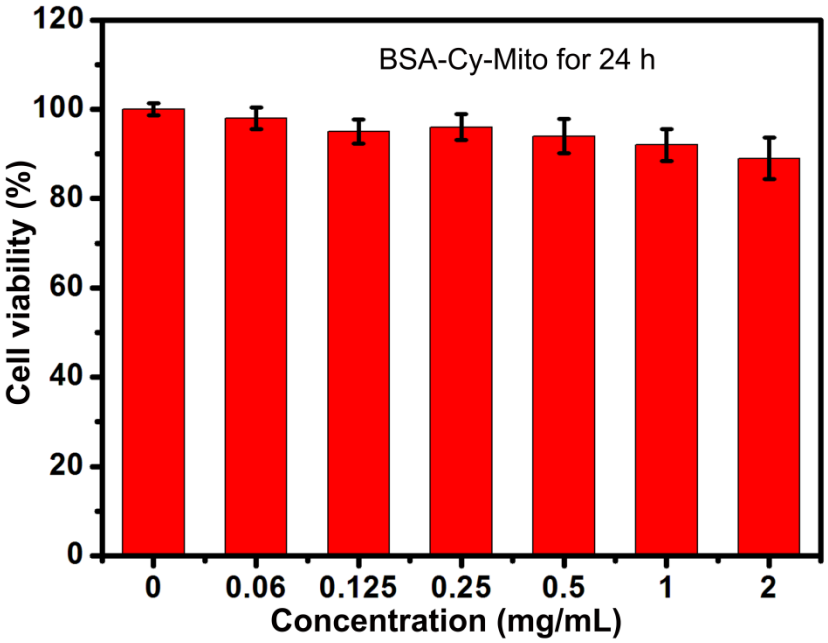

Figure S-6. Cell viabilities of the murine macrophage RAW 264.7 cells after incubated with various concentrations of BSA-Cy-Mito for 24 h.

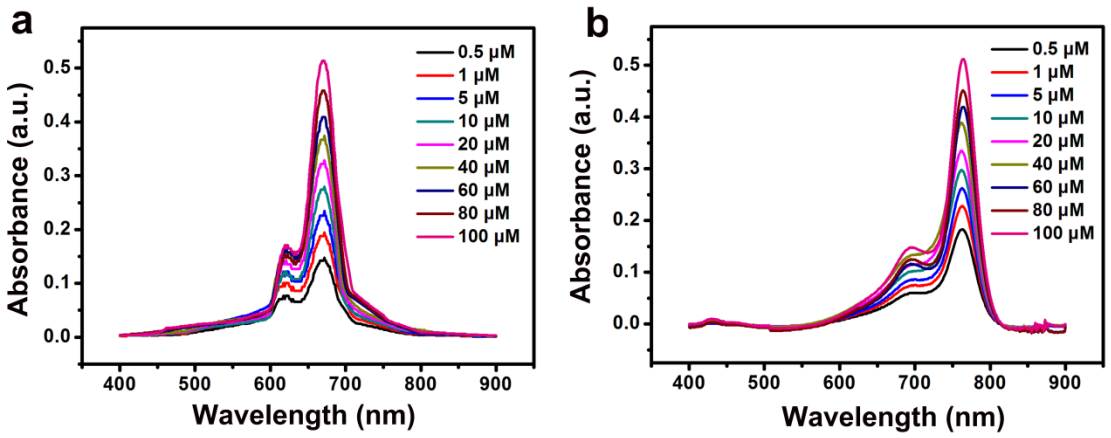

Figure S-7. UV-vis-NIR absorption spectra of BSA-Cy-Mito nanoprobe recorded in PBS buffers with different concentrations of (a) H_2O_2 and (b) GSH.

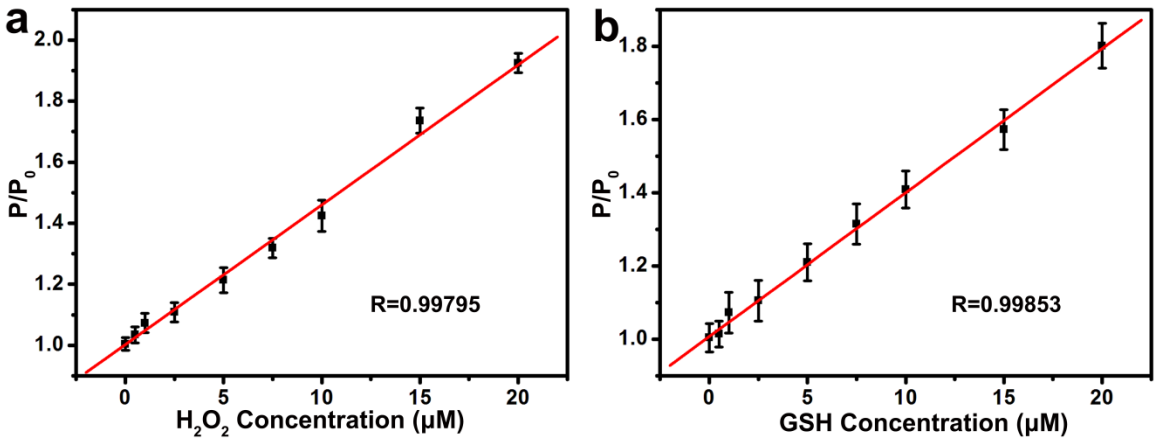

Figure S-8. Enhanced PA intensity (P/P_0) against the H_2O_2 and GSH concentration achieved by using a lower working concentration of the nanoprobe. From 0.5 μM to 20 μM, the linear equation for H_2O_2 was $P/P_0 = 0.04596 [H_2O_2] + 1.0031$, with a detection limit of 0.7 μM and coefficient R1 = 0.99795; the linear equation for GSH was $P/P_0 = 0.03931 [GSH] + 1.00706$, with a detection limit of 0.3 μM and coefficient R2 = 0.99853. Data are shown as the mean ± SD (n = 3).

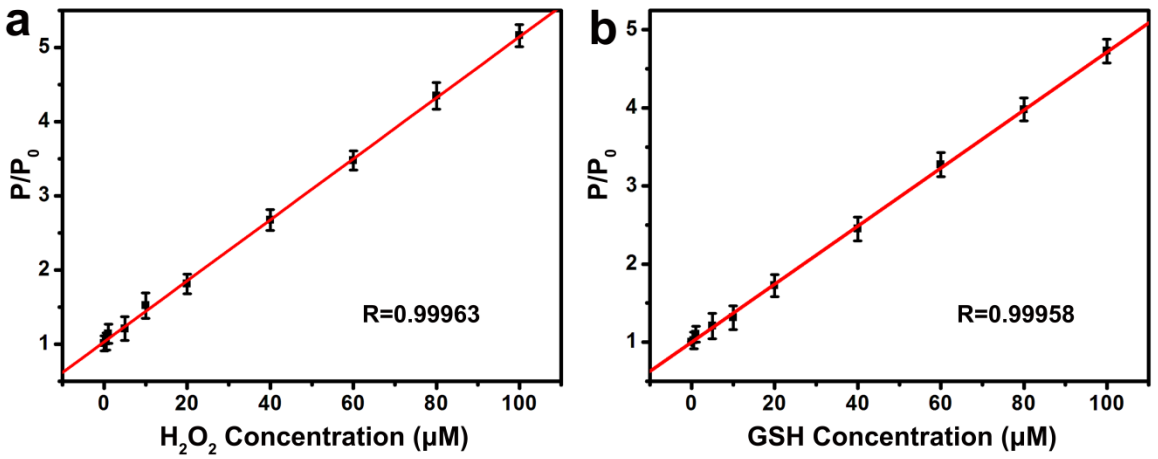

Figure S-9. Enhanced PA intensity (P/P_0) of the BSA-Cy-Mito nanoprobe toward H_2O_2 and GSH in the matrix of the plasma extract of catalase (100 μM) and BSO (5 mM) pretreated the murine macrophage RAW 264.7 cells. The linear equations were $P/P_0 = 0.04116 [H_2O_2] + 1.02983$ and $P/P_0 = 0.03707 [GSH] + 1.0128$, with coefficients R1 = 0.99963 and R2 = 0.99958. Data are shown as the mean ± SD (n = 3).

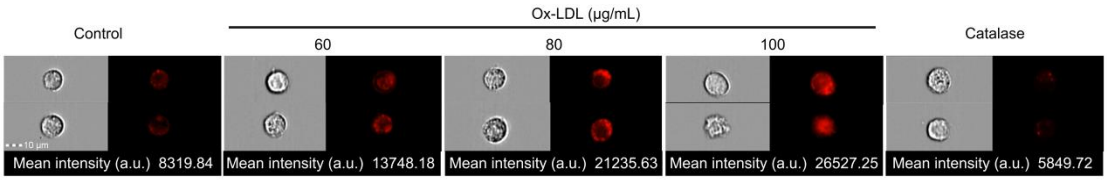

Figure S-10. Representative IFC images of the murine macrophage RAW 264.7 cells incubating with BSA-Cy-Mito nanoprobe (0.25 mg/mL) for 2 h after pretreating for 24 h with different concentrations of ox-LDL or catalase (100 μM).

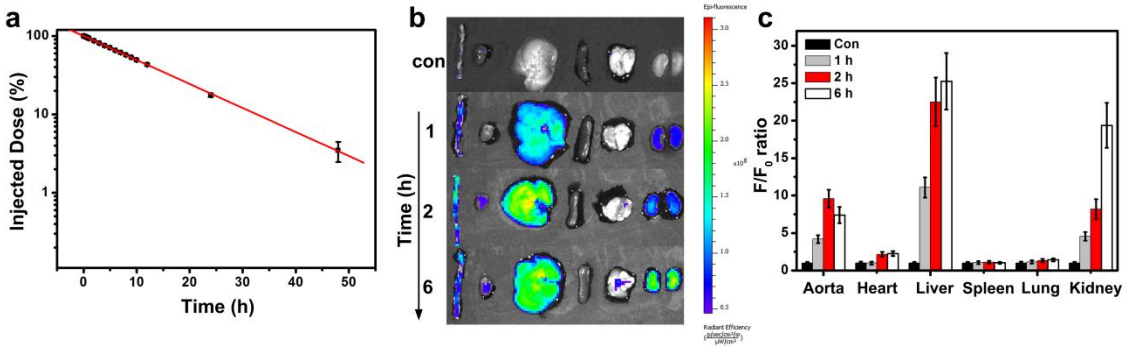

Figure S-11. (a) Pharmacokinetics of the BSA-Cy-Mito nanoprobe (10 mg/kg) after injection by vein. (b) Fluorescence images of the aortas and main organs of the plaque-bearing ApoE$^{-/-}$ mice sacrificed pre or post-injection of BSA-Cy-Mito (10 mg/kg) at 1, 2 and 6 h. (c) quantification of the fluorescence intensity in the tissue. Data are shown as the mean ± SD (n = 3).

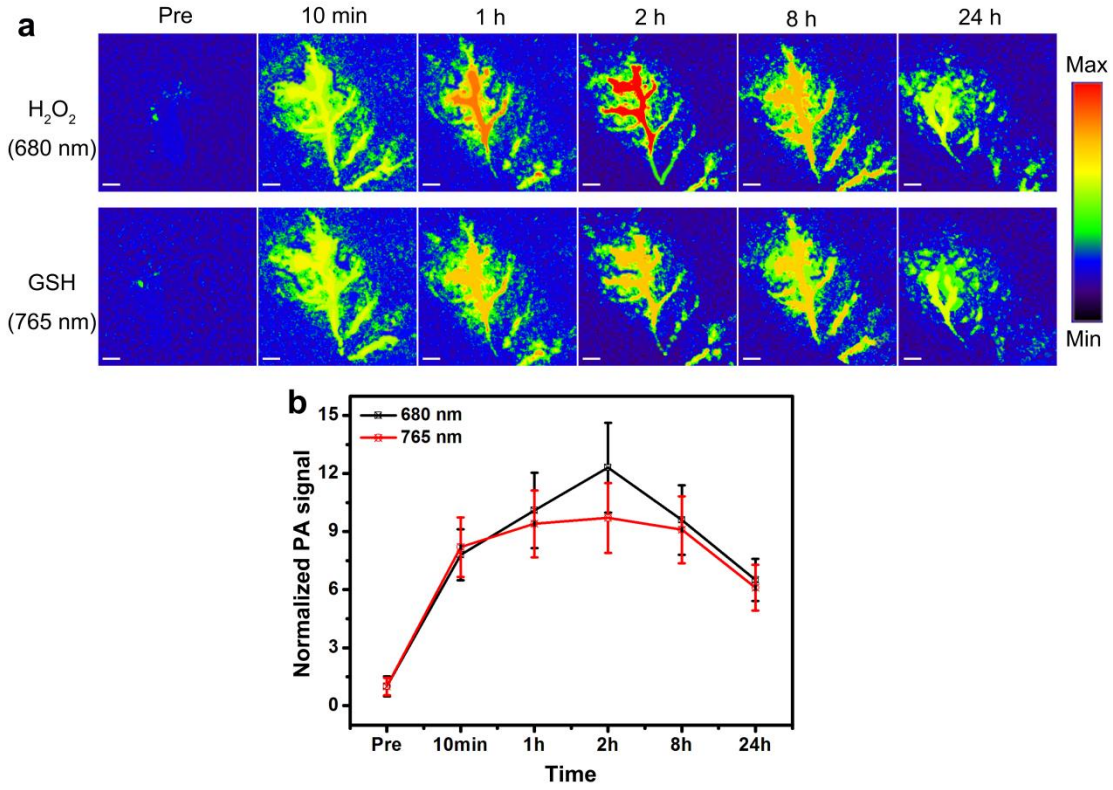

Figure S-12. PA imaging of abdominal aortas of plaque-bearing ApoE$^{-/-}$ mice after intravenously injected BSA-Cy-Mito (10 mg/kg) at different times (pre- and postinjection at 10 min, 1, 2, 8 and 24 h) under 680 and 765 nm pulse laser. Scale bar = 2 mm. Data are shown as the mean ± SD (n = 3).

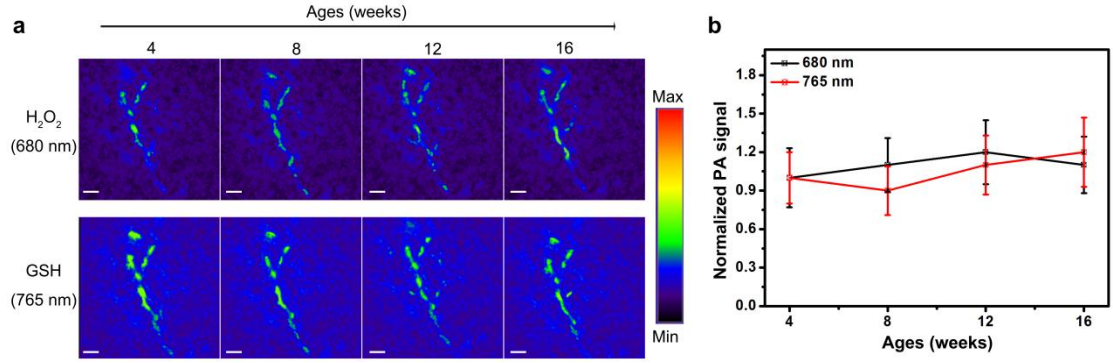

Figure S-13. PA imaging of abdominal aortas of healthy ApoE$^{-/-}$ mice in different ages (4, 8, 12 and 16 weeks) after intravenously injected BSA-Cy-Mito for 2 h under 680 and 765 nm pulse laser. Scale bar = 2 mm. Data are shown as the mean ± SD (n = 3).

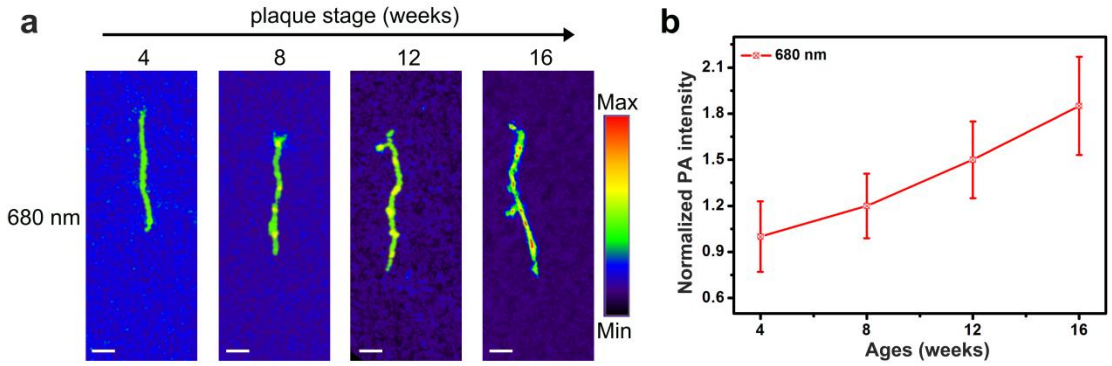

Figure S-14. *Ex vivo* PA imaging of the *en face* aorta in different plaque stages (4, 8, 12 and 16 weeks). Scale bar = 5 mm. Data are shown as the mean ± SD (n = 3).